

**SYNTHESIS, CHARACTERIZATION AND REACTIVITY
STUDIES OF ORGANOTIN ALKANESULFONATES**

PRIYANKA CHAUHAN



**DEPARTMENT OF CHEMISTRY
INDIAN INSTITUTE OF TECHNOLOGY DELHI**

JULY 2023

**SYNTHESIS, CHARACTERIZATION AND REACTIVITY
STUDIES OF ORGANOTIN ALKANESULFONATES**

by

PRIYANKA CHAUHAN

Submitted

**In fulfilment of the requirements of the degree of Doctor of Philosophy
to the**



**DEPARTMENT OF CHEMISTRY
INDIAN INSTITUTE OF TECHNOLOGY DELHI**

JULY 2023

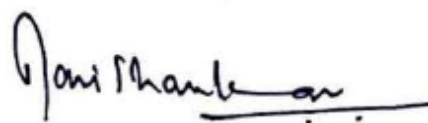
Dedicated to My Parents

CERTIFICATE

This is to certify that the thesis entitled “**SYNTHESIS, CHARACTERIZATION AND REACTIVITY STUDIES OF ORGANOTIN ALKANESULFONATES**” being submitted by Ms. Priyanka Chauhan to the Department of Chemistry, Indian Institute of Technology Delhi, for the award of the degree of Doctor of Philosophy is a record of bonafide research work carried out by her.

She has worked under my guidance and supervision and has fulfilled the requirements for the submission of the thesis, which to my knowledge has reached the requisite standard.

The results contained in this thesis have not been submitted in part or in full to any other University or Institute for the award of any degree or diploma.



Prof. Ravi Shankar

Department of Chemistry

Indian Institute of Technology Delhi

New Delhi-110016, India

ACKNOWLEDGEMENTS

By the divine providence of Almighty GOD, this is the time when my ship docks and I have the chance to sincerely thank all the people who helped me with my research. I did my best to compile a list of those who made significant contributions at this point, and I apologise if there were any omissions. Aside from my own efforts, the support and advice of many others play a significant role in the accomplishment of this thesis.

I would like to offer my sincere gratitude to my supervisor, Prof. Ravi Shankar, Department of Chemistry, Indian Institute of Technology Delhi, for his thorough direction, priceless recommendations, and ongoing encouragement. His prompt counsel, methodical approach, and rigorous scrutiny have provided the foundation for shaping my thesis in a successful direction. Even in the entire lockdown situation, I will always be grateful for his leadership, protection, and support. In addition, special thanks are due to the former and present Head of Chemistry Department, Prof. Narayanan Kurur and Prof. Siddharth Pandey for providing the necessary facilities for carrying out my research work.

The staff of the Instrumentation Laboratory of the Chemistry Department also deserves a special mention. I want to thank Mr. Alok, Ms. Shubra Gupta, and Mr. Narugopal Kuily for understanding the urgency of the results and assisting me in finishing the work on time. I would like to express my gratitude to Prof. Tanmay Dutta and Bipasa Dey for their help in antibacterial studies. Special thanks to Prof. Sartaj Tabassum (Chemistry Department, Aligarh Muslim University) for conducting the in vitro DNA interaction experiments. I acknowledge Pavletta Shestakova (Institute of Organic Chemistry and Center of Phytochemistry, Bulgarian Academy of Sciences) for solid state NMR studies. I especially like to thank Manish Kumar and Shubhangi for helping with the photoluminescence studies. Moreover, I would like to thank Prof. Gabriele Kociok-Köhn for the insightful conversation regarding crystallography. In the same vein, I owe DST-India and IIT Delhi for granting me access to the X-ray crystallographic machine.

Also, I would like to express my gratitude to IIT-Delhi for supporting me during my five years of research through the Junior Research and Senior Research Fellowships.

I convey special thanks to Dr. Ekta Jakhar, Dr. Nidhi Mahavar and Dr. Archishmati Dubey for their love, support, and care throughout this journey. I would like to thank Ragini Jain for her helpful suggestions during the course of the work. I owe a huge debt of gratitude to Aishwarya Chauhan and Akhilesh Mishra for lifting up my spirits in the hardest time of my life and for always being there as my support system. I also wish to thank Mr. Ashish Kumar for the moral support provided during this journey.

Finally, words are insufficient to convey my gratitude to my honorable parents, Mr. Rishi Pal Singh Chauhan and Mrs. Rekha Chauhan for their unwavering support, encouragement, and love. Words will never be able to adequately express my thanks to my loving father, who is unable to witness this day, for his priceless counsel and the seed of perseverance and determination he instilled in me. The irreparable loss can never be fixed but you will always remain inside my heart, as my hero. My elder sister and my brother-in-law Ankita and Vivek deserve the utmost gratitude for their steadfast love, support, and inspiration over the years. Last but not the least a special word of affection goes out to my nephew Viaan, whose grin motivates me to remain positive and work harder than ever to succeed in life.

Finally, I want to convey a special message to my parents for inspiring me to pursue my aspirations and reach new heights.

*सर्वतीर्थमयी माता सर्वदेवमयः पिता
मातरं पितरं तस्मात् सर्वयत्नेन पूजयेत्*

Priyanka
Priyanka Chauhan

ABSTRACT

The use of weakly coordinating oxy-sulfur anions such as triflate and arylsulfonates is quite prevalent in organotin coordination chemistry due to their varying degrees of sensitivity towards bonding with metal ions. Related chemistry derived from alkanesulfonate ligands is relatively new and provided an insight into the bonding nature of tin-sulfonate among this family and the structural attributes derived thereof. The work presented in the thesis is a systematic study to develop synthetic methods for anionic, cationic, and neutral organotin coordination frameworks associated with alkanesulfonate ligands. The stannate salts, $[n\text{-Bu}_4\text{N}][\text{R}_2\text{Sn}(\text{OSO}_2\text{R}^1)_3]$ ($\text{R} = n\text{-Bu, Ph; R}^1 = \text{Me, Et, } n\text{-Pr}$) are found to be promising candidates for this study being readily soluble in common organic solvents. The affinity of these ate complexes to undergo hydration/hydrolysis under ambient conditions has led to the isolation of salt cocrystals such as $[\text{Ph}_2\text{Sn}(\text{H}_2\text{O})_4][n\text{-Bu}_4\text{N}]_2[\text{OSO}_2\text{Me}]_4$ and $[n\text{-Bu}_2\text{Sn}(\text{H}_2\text{O})_4][n\text{-Bu}_4\text{N}][\text{OSO}_2\text{Et}]_3 \cdot \text{H}_2\text{O}$ which represent an unprecedented family comprising otherwise unstable tetra(aqua)diorganotin cations. The study has been extended to highlight potential antibacterial activity of these cocrystals against Gram-negative bacteria *Escherichia coli* (*E. coli*). Distinct behaviour of the stannate salts as a function of organic substituents on tin and /or sulfonate groups has been realized upon reaction with N-donor ligands. The illustrative examples include a cationic assembly, $[\text{Ph}_3\text{Sn}(\text{L})][\text{OSO}_2\text{Me}]$ ($\text{L} = 1,4\text{-bis}((1\text{H-imidazole-1-yl)methyl)benzene$) following dismutation of the phenyl groups and the salt cocrystal, $[n\text{-Bu}_4\text{N} \cdot \text{OSO}_2\text{Me} \cdot \text{H}_2\text{O}]_2[\{(n\text{-Bu}_2\text{Sn})_2(\text{OH})(\text{OSO}_2\text{Me})\}\text{O}]_2$ featuring tetraorganodistannoxane as the inorganic unit. The last chapter deals with a systematic study to address the role of solvothermal reactions in bringing about chemical transformation of $n\text{-Bu}_2\text{Sn}(\text{quin})\text{OSO}_2\text{Me}$ to $[(n\text{-Bu}_2\text{Sn} \cdot \text{quin})_2\text{SO}_4]$ via cleavage of the S-C bond. The bioinorganic aspect of these mixed-ligand di-*n*-butyltin sulfates has been delineated upon interaction with calf thymus-DNA.

प्राक्कथन

धातु आयनों के साथ संबंध के प्रति संवेदनशीलता की अलग-अलग डिग्री के कारण ऑर्गोटिन समन्वय रसायन विज्ञान में कमजोर समन्वय वाले ऑक्सी-सल्फर आयनों जैसे ट्राइफ्लेट और आर्यलसल्फोनेट्स का उपयोग काफी प्रचलित है। अल्केनसल्फोनेट से संबंधित रसायन विज्ञान अपेक्षाकृत नया है और इस परिवार के बीच टिन-सल्फोनेट की बॉन्डिंग प्रकृति और उसके द्वारा प्राप्त संरचनात्मक विशेषताओं में एक अंतर्दृष्टि प्रदान करता है। थीसिस में प्रस्तुत काम एल्केनसल्फोनेट लिगेंड से जुड़े आयनिक, धनिक और तटस्थ ऑर्गिनोटिन समन्वय ढांचे के लिए सिंथेटिक तरीकों को विकसित करने के लिए एक व्यवस्थित अध्ययन है। स्टैनेट लवण, $[n\text{-Bu}_4\text{N}][\text{R}_2\text{Sn}(\text{OSO}_2\text{R}^1)_3]$ ($\text{R} = n\text{-Bu, Ph; R}^1 = \text{Me, Et, } n\text{-Pr}$) इस अध्ययन के लिए आशाजनक उम्मीदवार पाए जाते हैं जो आम कार्बनिक सॉल्वेंट्स में आसानी से घुलनशील होते हैं। परिवेशी परिस्थितियों में हाइड्रेशन/हाइड्रोलिसिस से गुजरने के लिए इन एट कॉम्प्लेक्स की आत्मीयता ने साल्ट कोक्रिस्टल के अलगाव को जन्म दिया है जैसे कि $[\text{Ph}_2\text{Sn}(\text{H}_2\text{O})_4][n\text{-Bu}_4\text{N}]_2[\text{OSO}_2\text{Me}]_4$ और $[n\text{-Bu}_2\text{Sn}(\text{H}_2\text{O})_4][n\text{-Bu}_4\text{N}][\text{OSO}_2\text{Et}]_3 \cdot \text{H}_2\text{O}$ जो एक अभूतपूर्व परिवार का प्रतिनिधित्व करता है जिसमें अन्यथा अस्थिर टेट्रा (एक्वा) डायऑर्गिनोटिन कैटाइअन शामिल हैं। ग्राम-नकारात्मक बैक्टीरिया *Escherichia coli* (*E. coli*). के खिलाफ इन कोक्रिस्टल की संभावित जीवाणुरोधी गतिविधि को उजागर करने के लिए अध्ययन का विस्तार किया गया है। टिन और / या सल्फोनेट समूहों पर कार्बनिक पदार्थों के कार्य के रूप में स्टैनेट लवणों का विशिष्ट व्यवहार N-डोनर लिगेंड्स के साथ प्रतिक्रिया पर महसूस किया गया है। उदाहरण में Phenyl समूहों के विघटन के बाद कैटाइअनिक असेंबली $[\text{Ph}_3\text{Sn}(\text{L})][\text{OSO}_2\text{Me}]$ और अकार्बनिक यूनिट के रूप में टेट्राऑर्गिनोडिस्टैनोक्सेन साल्ट कोक्रिस्टल $[n\text{-Bu}_4\text{N} \cdot \text{OSO}_2\text{Me} \cdot \text{H}_2\text{O}]_2 \{[(n\text{-Bu}_2\text{Sn})_2(\text{OH})(\text{OSO}_2\text{Me})]\text{O}\}_2$ शामिल हैं। अंतिम अध्याय में S-C बॉन्ड के दरार के माध्यम से $n\text{-Bu}_2\text{Sn}(\text{quin})\text{OSO}_2\text{Me}$ से $[(n\text{-Bu}_2\text{Sn} \cdot \text{quin})_2\text{SO}_4]$ के रासायनिक परिवर्तन को लाने में सॉल्वोथर्मल प्रतिक्रियाओं की भूमिका को संबोधित करने के लिए एक

व्यवस्थितअध्ययन से संबंधित है। इन मिश्रित-लिगेण्ड $[(n\text{-Bu}_2\text{Sn}\cdot\text{quin})_2\text{SO}_4]$ के जैव-कार्बनिक पहलू को calf thymus-DNA पर चित्रित किया गया है।

CONTENTS

	Page No.
<i>Certificate</i>	i
<i>Acknowledgments</i>	ii–iii
<i>Abstract</i>	iv–vi
<i>Table of contents</i>	vii
<i>List of Figures</i>	viii–xi
<i>List of Tables</i>	xii–xiii
<i>List of Schemes</i>	xiv–xv
<i>Glossary of Symbols and Abbreviations</i>	xvi–xvii
CHAPTER 1	
Introduction	1–13
Scope and aim	13–14
CHAPTER 2	
Materials and methods	15–29
CHAPTER 3	
Synthesis and hydrolysis behavior of diorganostannate salts – Approach to salt cocrystals of tetra(aqua)diorganotin cations.	30–56
CHAPTER 4	
Reactivity studies of diorganostannates, [n-Bu₄N][R₂Sn(OSO₂R¹)₃] (R = Ph, n-Bu; R¹ = Me, Et) with N-donor ligands.	57–85
CHAPTER 5	
Diorganotin coordination polymers incorporating carboxylate/ methanesulfonate/ sulfate ligands and their <i>in vitro</i> bioactivity studies.	86–109
SUMMARY	110–116
REFERENCES	117–128
APPENDIX	
Figures and Tables	129–148
BIODATA OF THE AUTHOR	149–152

LIST OF FIGURES

Figure No.	Description	Page No.
Chapter 1		
1.1	Coordination modes of the carboxylate group.	10
1.2	Structures of (a) $\text{Me}_2\text{Sn}(\text{O}_2\text{CCH}_3)_2$ (b) $\text{Me}_2\text{Sn}(\text{O}_2\text{CH})_2$ (c) $(\text{cyclo-hex})_3\text{Sn}(\text{OAc})$, (d) $\text{Bz}_3\text{Sn}(\text{OAc})$ and (e) $\text{Ph}_2\text{EtSn}(\text{OAc})$.	10
1.3	Illustrative examples of polytopic carboxylic acids.	11
Chapter 3		
3.1	ESI-MS of $[\textit{n}\text{-Bu}_4\text{N}][\textit{n}\text{-Bu}_2\text{Sn}(\text{OSO}_2\text{Et})_3]$ (2) and $[\textit{n}\text{-Bu}_4\text{N}][\text{Ph}_2\text{Sn}(\text{OSO}_2\text{Et})_3]$ (5).	38
3.2	$^{13}\text{C}\{^1\text{H}\}$ NMR spectrum of $[\textit{n}\text{-Bu}_4\text{N}][\textit{n}\text{-Bu}_2\text{Sn}(\text{OSO}_2\text{Me})_3]$ (1)	39
3.3	$^{119}\text{Sn}\{^1\text{H}\}$ NMR spectra of (a) $[\textit{n}\text{-Bu}_4\text{N}][\textit{n}\text{-Bu}_2\text{Sn}(\text{OSO}_2\text{Me})_3]$ (1) and (b) $[\textit{n}\text{-Bu}_4\text{N}][\text{Ph}_2\text{Sn}(\text{OSO}_2\text{Me})_3]$ (4).	39
3.4	ORTEP (30% probability) with numbering scheme for (a) $[\textit{n}\text{-Bu}_4\text{N}][\textit{n}\text{-Bu}_2\text{Sn}(\text{OSO}_2\text{Me})_3]$ (1) and (b) $[\textit{n}\text{-Bu}_4\text{N}][\textit{n}\text{-Bu}_2\text{Sn}(\text{OSO}_2\text{Et})_3]$ (2).	41
3.5	ORTEP (30% probability) with numbering scheme for $[\textit{n}\text{-Bu}_4\text{N}][\text{Ph}_2\text{Sn}(\text{OSO}_2\text{Me})_3]$ (4) and (b) $[\textit{n}\text{-Bu}_4\text{N}][\text{Ph}_2\text{Sn}(\text{OSO}_2\text{Et})_3]$ (5).	42
3.6	(a) ORTEP (30% probability) with numbering scheme for $[\textit{n}\text{-Bu}_2\text{Sn}(\text{H}_2\text{O})_4][\textit{n}\text{-Bu}_4\text{N}][\text{OSO}_2\text{Et}]_3 \cdot \text{H}_2\text{O}$ (7). (b) Extended 2D view. (c) Space filling model of the lamellar structure.	47
3.7	(a) ORTEP (30% probability) with numbering scheme for $[\textit{n}\text{-Bu}_2\text{Sn}(\mu\text{-OH})(\text{H}_2\text{O})_2]_2[\textit{n}\text{-Bu}_4\text{N}]_2[\text{OSO}_2\text{Pr}]_4$ (8). (b) Extended 2D view.	50
3.8	ORTEP (30% probability) with numbering scheme for $[\text{Ph}_2\text{Sn}(\text{H}_2\text{O})_4][\textit{n}\text{-Bu}_4\text{N}]_2[\text{OSO}_2\text{Me}]_4$ (9).	51

Figure No.	Description	Page No.
3.9	ORTEP (30% probability) with numbering scheme for $[\text{Ph}_2\text{Sn}(\text{H}_2\text{O})_4][n\text{-Bu}_4\text{N}]_3[\text{OSO}_2\text{Et}]_5 \cdot 3\text{H}_2\text{O}$ (10).	51
3.10	$^{119}\text{Sn}\{^1\text{H}\}$ NMR spectra of (a) $[n\text{-Bu}_2\text{Sn}(\text{H}_2\text{O})_4][n\text{-Bu}_4\text{N}][\text{OSO}_2\text{Et}]_3 \cdot \text{H}_2\text{O}$ (7) and (b) $[\text{Ph}_2\text{Sn}(\text{H}_2\text{O})_4][n\text{-Bu}_4\text{N}]_2[\text{OSO}_2\text{Me}]_4$ (9).	53
3.11	(a) Percentage survival of <i>E. coli</i> bacteria as a function of concentration of $[n\text{-Bu}_2\text{Sn}(\text{H}_2\text{O})_4][n\text{-Bu}_4\text{N}][\text{OSO}_2\text{Et}]_3 \cdot \text{H}_2\text{O}$ (7). (b) Inhibition zone for 7 at different concentrations.	54
Chapter 4		
4.1	Structures of the N-donor ligands.	59
4.2	ESI-MS of $[n\text{-Bu}_4\text{N}][\text{Ph}_2\text{Sn}(\text{OSO}_2\text{Me})_3]$ (4).	61
4.3	(a) ORTEP (30% probability) with numbering scheme for $[\text{Ph}_3\text{Sn}(\text{bix})][\text{OSO}_2\text{Me}]$ (11). (b) Extended 2D view. (c) Space filling model of the lamellar structure.	64
4.4	(a) ORTEP (30% probability) with numbering scheme for $[\text{Ph}_3\text{Sn}(\text{OSO}_2\text{Me})\text{H}_2\text{O}][4,4'\text{-bipy}]$ (12). (b) Extended 2D view <i>via</i> N-H---O and C-H---O hydrogen bonding interactions.	64
4.5	(a) Perspective view of (a) $\text{Ph}_3\text{SnOSO}_2\text{Me}$ (13) and (b) $\text{Ph}_2\text{Sn}(\text{OSO}_2\text{Me})_2 \cdot 2,2'\text{-bipy}$ (14) along with atomic numbering scheme.	65
4.6	$^{119}\text{Sn}\{^1\text{H}\}$ NMR spectra of (a) $[\text{Ph}_3\text{Sn}(\text{bix})][\text{OSO}_2\text{Me}]$ (11) and (b) $\text{Ph}_2\text{Sn}(\text{OSO}_2\text{Me})_2 \cdot 2,2'\text{-bipy}$ (14)	69
4.7	(a) Normalized PL spectra of (a) <i>bix</i> and 11 ($\lambda_{\text{ex}} = 375$ nm) (b) <i>4,4'</i> - <i>bipy</i> and 12 ($\lambda_{\text{ex}} = 365$ nm) in solid state.	70
4.8	ESI-MS of $[n\text{-Bu}_4\text{N}][n\text{-Bu}_2\text{Sn}(\text{OSO}_2\text{Me})_3]$ (1).	71
4.9	Two-dimensional supramolecular assembly of $[\{(n\text{-Bu}_2\text{Sn})_2(\text{OH})(\text{OSO}_2\text{Me})\text{O}\}_2]$ (15).	75
4.10	ORTEP (30% probability) and numbering scheme for $[n\text{-Bu}_4\text{N} \cdot \text{OSO}_2\text{Me} \cdot \text{H}_2\text{O}]_2[\{(n\text{-Bu}_2\text{Sn})_2(\text{OH})(\text{OSO}_2\text{Me})\text{O}\}_2]$ (16).	75
4.11	ORTEP (30% probability) and numbering scheme for <i>n</i> -	

Figure No.	Description	Page No.
	$\text{Bu}_2\text{Sn}(\text{OSO}_2\text{Me})_2 \cdot 2,2'$ -bipy (17).	76
4.12	(a) ORTEP (30% probability) and numbering scheme for n - $\text{Bu}_2\text{Sn}(\text{OSO}_2\text{Et})_2 \cdot \text{bix}$ (19). (b) Two-dimensional view in the bc plane. (c) space filling model along ab plane.	76
4.13	(a) $^{119}\text{Sn}\{^1\text{H}\}$ NMR spectrum (solid state) and (b) in solution of $[\{(n\text{-Bu}_2\text{Sn})_2(\text{OH})(\text{OSO}_2\text{Me})\}\text{O}]_2$ (15).	80
4.14	(a) ORTEP (30% probability) and numbering scheme for $[\text{H}_2\text{bix}][n\text{-Bu}_4\text{N}]_2[\text{OSO}_2\text{Me}]_4$ (15a). Two-dimensional motif of $[\text{H}_2\text{bix}][\text{OSO}_2\text{Me}]_2$. (c) Three-dimensional view of 15a .	83
4.15	(a) ORTEP (30% probability) and numbering scheme for $[\text{H}_2 4,4'\text{-bipy}][\text{OSO}_2\text{Me}]_2$ (16a). (b) Two-dimensional view via N-H---O and C-H---O hydrogen bonding interactions.	83
Chapter 5		
5.1	Structures of N-heteroaromatic carboxylic acids.	88
5.2	ESI-MS of $[\{n\text{-Bu}_2\text{Sn}(\text{O}_2\text{CC}_9\text{H}_6\text{N-2})\}_2\text{SO}_4]$ (21).	91
5.3	ORTEP (30% probability) of $[n\text{-Bu}_2\text{Sn}(\text{O}_2\text{CC}_9\text{H}_6\text{N-2})\text{OSO}_2\text{Me}]$ (21a).	92
5.4	ORTEP (30% probability) of (a) $[n\text{-Bu}_2\text{Sn}(\text{O}_2\text{CC}_9\text{H}_6\text{N-2})]_2\text{SO}_4$ (21) (b) extended polymeric chain of $[n\text{-Bu}_2\text{Sn}(\text{O}_2\text{C-4-OMe-C}_9\text{H}_6\text{N-2})]_2\text{SO}_4$ (22) along b -axis.	94
5.5	ORTEP (30% probability) of $[n\text{-Bu}_2\text{Sn}(\text{O}_2\text{CC}_5\text{H}_3\text{NCOOEt})_2 \cdot \text{H}_2\text{O}]$ (23).	99
5.6	ORTEP (30% probability) of $[n\text{-Bu}_2\text{Sn}(\text{O}_2\text{CC}_5\text{H}_3\text{OH})_2 \cdot \text{H}_2\text{O}] \cdot \text{EtOH}$ (24).	99
5.7	IR spectrum of $[n\text{-Bu}_2\text{Sn}(\text{O}_2\text{CC}_5\text{H}_3\text{NCOOEt})_2 \cdot \text{H}_2\text{O}]$ (23).	102
5.8	UV-visible spectra of (a) 21 and (b) 22 upon addition of increasing concentration of ct-DNA in aqueous saline tris HCl buffer.	105
5.9	Emission spectra of EB+DNA system upon interaction with increasing concentration of 21 and 22 .	105
5.10	pBR322 cleavage bands observed for (a) 21 and (b) 22 [Lane	

Figure No.	Description	Page No.
	1 = DNA control, Lane 2 (2.5 μ M) to 9 (20 μ M)].	106
5.11	Docked pose of 21 with DNA.	107
5.12	Docked pose of 22 with DNA.	107

Summary

S1	Molecular structure of $[\text{Ph}_2\text{Sn}(\text{H}_2\text{O})_4][n\text{-Bu}_4\text{N}]_2[\text{OSO}_2\text{Me}]_4$ (9).	112
S2	Layered structure of $[\text{Ph}_3\text{Sn}(\text{bix})][\text{OSO}_2\text{Me}]$ (11).	113
S3	Perspective view of $[n\text{-Bu}_2\text{Sn}(\text{O}_2\text{CC}_5\text{H}_3\text{NCOOEt})_2 \cdot \text{H}_2\text{O}]$ (23).	115

Appendix

A1	TGA of the stannate salts, 1-5 .	131
A2	Perspective view of $n\text{-Bu}_2\text{Sn}(\text{OH})\text{OSO}_2\text{Me}$ (6).	132
A3	TGA of compounds 11-14 .	137
A4	IR spectra of 11 and 12 .	139
A5	Lifetime emission for 11 and 12 .	140
A6	TGA of compounds, 15-17 and 19 .	141
A7	TGA of compounds, 21 and 22 .	146

LIST OF TABLES

Table No.	Description	Page No.
Chapter 3		
3.1	ESI-MS and ^{119}Sn NMR data of $[n\text{-Bu}_4\text{N}][\text{R}_2\text{Sn}(\text{OSO}_2\text{R}^1)_3]$ ($\text{R} = n\text{-Bu}$, $\text{R}^1 = \text{Me}$ (1), Et (2), $n\text{-Pr}$ (3); $\text{R} = \text{Ph}$, $\text{R}^1 = \text{Me}$ (4), Et (5)).	37
3.2	Selected bond lengths (\AA) and angles ($^\circ$) for 1 and 2 .	43
3.3	Selected bond lengths (\AA) and angles ($^\circ$) for 4 and 5 .	44
3.4	Selected bond lengths (\AA) and angles ($^\circ$) for 7 .	48
Chapter 4		
4.1	Selected bond lengths [\AA] and angles [$^\circ$] for 11 .	66
4.2	Selected bond lengths [\AA] and angles [$^\circ$] for 12 .	66
4.3	Selected bond lengths [\AA] and angles [$^\circ$] for 13 .	67
4.4	Selected bond lengths [\AA] and angles [$^\circ$] for 14 .	67
4.5	Selected bond lengths [\AA] and angles [$^\circ$] for 15 .	78
4.6	Selected bond lengths [\AA] and angles [$^\circ$] for 16 .	78
4.7	Selected bond lengths [\AA] and angles [$^\circ$] for 17 .	79
4.8	Selected bond lengths [\AA] and angles [$^\circ$] for 19 .	79
4.9	Reaction conditions: ROH (9.1 mmol), $(\text{CH}_3\text{CO})_2\text{O}$ (1.0 mL). [a] Isolable yield after usual workup. Identified by ^{13}C NMR spectroscopy.	81
Chapter 5		
5.1	Selected bond lengths [\AA] and angles [$^\circ$] for 21a .	95
5.2	Selected bond lengths [\AA] and angles [$^\circ$] for 21 .	95

5.3	Selected bond lengths [\AA] and angles [$^{\circ}$] for 22 .	96
5.4	Selected bond lengths [\AA] and angles [$^{\circ}$] for 23 .	100
5.5	Selected bond lengths [\AA] and angles [$^{\circ}$] for 24 .	101
Summary		
S1	Summary of the coordination frameworks.	116
Appendix		
A1	Summary of the crystallographic data for [<i>n</i> - Bu ₄ N][R ₂ Sn(OSO ₂ R ¹) ₃] [R = <i>n</i> -Bu, R ¹ = Me (1), Et (2), R = Ph, R ¹ = Me (4), Et(5)].	130
A2	Summary of Crystallographic data of 7-10 .	133
A3	Selected bond lengths (\AA) and angles ($^{\circ}$) for 8 .	134
A4	Selected bond lengths [\AA] and angles [$^{\circ}$] for 9 .	135
A5	Selected bond lengths [\AA] and angles [$^{\circ}$] for 10 .	136
A6	Summary of Crystallographic data of 9-12 .	138
A7	Summary of Crystallographic data of 15-17 and 19 .	142
A8	Summary of Crystallographic data of 15a and 16a .	143
A9	Selected bond lengths [\AA] and angles [$^{\circ}$] for 15a .	144
A10	Selected bond lengths [\AA] and angles [$^{\circ}$] for 16a .	145
A11	Summary of the crystallographic data for 21a , 21 and 22 .	147
A12	Summary of Crystallographic data of 23 and 24 .	148

LIST OF SCHEMES

Scheme No.	Description	Page No.
Chapter 1		
1.1	Synthesis of diorganotin triflates.	4
1.2	Probable mechanism for the formation of distannoxane.	4
1.3	Di-/triorganotin cations with pincer ligands.	6
1.4	Diorganotin phosphonate clusters with appended sulfonate groups.	9
1.5	Hydrolysis products of $R_2Sn(OR^1)(OSO_2R^1)$.	9
1.6	Reticular synthesis of dicarboxylato-tetramethyldistannoxanes.	12
Chapter 3		
3.1	Proposed mechanism for the formation of diorganostannates, 1-5 .	35
3.2	Synthesis of salt cocrystals, 7-10 .	45
Chapter 4		
4.1	Synthesis of compounds, 11-14 .	60
4.2	Synthesis of compounds, 15-19 .	72
Chapter 5		
5.1	Synthesis of compounds, 21 and 22 .	89
5.2	Proposed mechanism for the formation of 21 .	90
5.3	Synthesis of compounds, 23-25 .	97
Summary		

S1	Synthesis of the salt cocrystals, 7-10 .	111
S2	Synthesis of compounds, 11-14 .	113

GLOSSARY OF SYMBOLS AND ABBREVIATIONS

General Abbreviations

ORTEP	Oak Ridge Thermal Ellipsoid Plot	CP MAS	Cross Polarization Magic Angle Spinning
PDB	Protein Data Bank	OTf	Triflate
OAc	Acetate	ct-DNA	Calf thymus-DNA
THF	Tetrahydrofuran	pic	picolinate
DMSO	Dimethyl sulfoxide	quin	quinaldate
EB	Ethidium bromide	Hex	Hexyl
<i>n</i> -Bu	<i>n</i> -Butyl	<i>t</i> -Bu	<i>t</i> -Butyl
Et	Ethyl	Me	Methyl
Ph	Phenyl	Bu	Butyl
<i>n</i> -Pr	<i>n</i> -Propyl	<i>m</i> -	Meta-
<i>o</i> -	Ortho-	<i>p</i> -	Para-
4,4'-bipy	4,4'-Bipyridine	2,2'-bipy	2,2'-Bipyridine
pyr	Pyrazine	bix	1,4-bis((1H-imidazole-1-yl)methyl)benzene
HMPA	Hexamethylphosphoramide	<i>K</i> _{sv}	Stern-Volmer constant
ϵ	Extinction coefficient	<i>pK</i> _a	Acidity constant
<i>K</i> _b	Binding constant	Hz	Hertz
b.p.	boiling point	Σ	Sum
g	gram	ns	Nanosecond
%	Percent	I	Fluorescence intensity
rt	Room temperature	h	Hour
Obsd.	Observed	Calcd.	Calculated
Eqn	Equation	V	Voltage
μ	Micro	Δ	Difference
mmol	Millimole	M	Molar concentration
°C	Degree centigrade	Bz	Benzyl

Molecular Structure Determination

a, b, c	Unit cell dimensions	Z	Number of molecules in the unit cell
Å	Angstrom	F(000)	Number of electrons in the unit cell
°	Degree	μ	Absorption coefficient
V	Volume of the Unit cell	ρ	Density
α, β, γ	Unit cell angles		

Spectroscopy

TGA	Thermogravimetric analysis	UV	Ultraviolet
ESI	Electrospray Ionization	Vis	Visible
m/z	Mass per charge	J	Coupling constant
NMR	Nuclear magnetic resonance	δ	Chemical shift
IR	Infrared	ν	Frequency
FT	Fourier transform	λ	Wavelength
PL	Photoluminescence	s	singlet
sym	Symmetric	d	doublet
asym	Asymmetric	t	triplet
ppm	Parts per million	m	multiplet
A	Absorbance	q	quadrat